Polym. Bull. (2012) 69:273–289
DOI 10.1007/s00289-012-0710-5

ORIGINAL PAPER

Synthesis and characterization of new polyfluorene derivatives: using phenanthro[9,10-*d*]imidazole group as a building block for deep blue light-emitting polymer

Zhiming Wang · Zhao Gao · Shanfeng Xue · Yulong Liu · Wensi Zhang · Cheng Gu · Fangzhong Shen · Ping Lu · Yuguang Ma

Received: 30 September 2011 / Revised: 27 November 2011 / Accepted: 20 January 2012 /
Published online: 1 February 2012

Abstract A series of novel polyfluorene derivatives **P1/4**, **P2/4**, and **P3/4**, containing phenanthro[9,10-d]imidazole group on backbone are designed, synthesized, and well characterized. They all show high-molecular weights, good solubilities, and excellent thermal stabilities. The CV results of all three compounds show the lower LUMO levels and higher HOMO levels than **PF**. Among them, **P3/4** exhibits deep blue emission both in solution and in solid state. The PLED based on **P3/4** shows higher device performance and locates in the deep blue region with a CIE coordinate of (0.17, 0.08).

Keywords Deep blue emission · Phenanthrenequinone · Imidazole · Multifunctional · Polymer

Introduction

Conjugated polymer-based electroluminescent devices are of growing interest in display applications because they can be made by spin-coating or inkjet printing technologies [1–8]. Remarkable progress has been made in achieving high-quality polymers that emit various colors in the past decade [9–13]. One of the remaining challenges is to develop polymers for achieving deep blue emission with high efficiency since the performance of deep blue polymer light emitting diodes

Z. Wang · Z. Gao · S. Xue · Y. Liu · W. Zhang · C. Gu · F. Shen · P. Lu (✉) · Y. Ma
State Key Laboratory of Supramolecular Structure and Materials, Jilin University,
2699 Qianjin Avenue, Changchun 130012, People's Republic of China
e-mail: lup@jlu.edu.cn

Z. Wang
School of Petrochemical Engineering, Shenyang University of Technology,
Liaoyang
111003, People's Republic of China

(PLEDs) is relatively low behind. Unbalanced charge injection and transport is one of the major problems. The high-energy gap essential for deep blue light emitting polymer often results in low electron affinities, which hampers the electron injection and the balance of the charge carriers [14, 15]. To solve the problem, multilayered structure which constitutes an electron transport layer, an emitting layer and a hole transport layer are widely applied to improve the performance of the devices [16–21]. But the sequential deposition of these layers provides additional complexity and the cost of such devices will be increased. Thus, the pursuit for new and multifunctional deep blue emitter with good charge injection properties remains as one of the most active areas in this field [22–25].

Most conjugated molecules are p-type due to their inherent richness of π electrons which causes the unbalanced injection and transport of carriers [26, 27]. Thus, n-type unit is often introduced to increase the electron injection and transport property [28–31]. In recent years, imidazole derivatives are found to be an important functional group for adjusting the LUMO energy level [32]. For example, benzoimidazole-based compound 1,3,5-tris(*N*-phenylbenzimidazol-2-yl)benzene (TPBi), which has a LUMO level of −2.40 eV, have been widely used in OLEDs as electron injection layer. Generally speaking, when the LUMO level of a compound is lowered to enhance the electron injection and transport ability, the HOMO level will be decreased at the same time, leading to higher hole-injection barrier. Thus, TPBi also can be used as hole blocking layer but not as the emitting layer [33, 34]. Our group have designed and synthesized a new multifunctional compound BPPI, in which benzoimidazole unit in TPBi is replaced by phenanthro[9,10-*d*]imidazole (PI) unit to enhance the holes injection and transport ability. BPPI exhibits excellent thermal stability, highly efficient fluorescence, and more balanced carrier injection [35]. The double-layered device based on BPPI shows higher maximum luminance and lower turn-on voltage than the multilayered one which has an independent electron injection layer. Because of the adjustment of the carriers injection property as well as deep blue emission by PI, we thought it might be a good building block for deep blue light emitting polymer. In this article, we report three polyfluorene derivatives containing PI unit on backbone. Fluorene was chosen as the building block because of its blue emission, good solubility, and high efficiency [36, 37]. These polymers show good blue or deep blue fluorescence emission. Compared with polyfluorene, the thermodynamic properties have significantly increased. And they all show lower LUMO levels and higher HOMO energy levels compared with **PF**, exhibiting more balanced carrier injection property. The performance of double-layered device of **P3/4** shows higher efficiency than **PF** and deep blue emission with a CIE coordinate of (0.17, 0.08).

Experimental section

Materials and instrumentation

Tetrahydrofuran (THF) was distilled under normal pressure from sodium benzophenone ketyl under nitrogen immediately prior to use. Other solvents of high

purities were used without further purification. $Pd(PPh_3)_4$ was purchased from Aldrich and used as received. 2,7-dibromo-9,9-dihexylfluorene, 4,4,4′,4′,5,5,5′,5′-hexyl-2,2′-bi(1,3,2-dioxaborolane), and 2,7-dibromophenanthrenequinone were synthesized according to our previous published procedures [35–39]. IR spectra were recorded on a Perkin-Elmer 16 PC FT-IR spectrophotometer. ^{1}H NMR spectra were measured on an AVANCZ 500 spectrometer using chloroform-*d* ($CDCl_3$) or dimethylsulfoxide as solvents and tetramethylsilane ($\delta = 0$ ppm) as internal standard. The MALDI-TOF MS were recorded using an AXIMA-CFR™ plus instrument. UV–Vis absorption spectra were measured on a UV-3100 spectrophotometer. Thermogravimetric analysis (TGA) of the polymers was evaluated on a TA TGA Q500 instrument under nitrogen at a heating rate of 20 °C/min. The photoluminescence (PL) spectra were recorded on a RF-5301PC spectrofluorometer. The PL quantum yields (Φ_f) were estimated using quinine sulfate ($\Phi_f = 54\%$ in 0.1 M sulfuric acid) as reference in THF. Weight (M_w) and number average (M_n) molecular weights and polydispersity indices (M_w/M_n) of the polymers were estimated by a Waters Associates gel permeation chromatography system equipped with refractive index and UV detectors. THF was used as eluent at a flow rate of 1.0 mL/min. A set of monodisperse polystyrene standards covering molecular weight range of 10^3–10^7 was used for the molecular weight calibration. Cyclic voltammetry (CV) were performed with a BAS 100 W Bioanalytical Systems, using a glass carbon disk ($\Phi = 3$ mm) as working electrode, platinum wire as auxiliary electrode, with porous ceramic wick, Ag/Ag^+ as reference electrode, standardized for the redox couple ferricinium/ferrocene.

Monomer synthesis

Polufluorene's monomer **M4** is synthesized according to our previous published procedures [36], whereas compounds **M1**, **M2**, and **M3**, are prepared according to the synthetic routes shown in Scheme 1. Typical experimental procedures for their syntheses are shown below.

Preparation of 3,4-bis(hexyloxy)benzaldehyde

To a 250 mL round-bottom flask equipped with a stirrer were added 2.80 g (20.0 mmol) of 3,4-dihydroxybenzaldehyde, 4.10 g (30.0 mmol) of K_2CO_3, 8.00 g (50 mmol) of bromohexane and CH_3CN (100 mL). After refluxing for 48 h, the reaction was stopped by adding dilute hydrochloric acid (HCl). The mixture was then washed with water, extracted by $CHCl_3$ and dried over $MgSO_4$. The filtrates were collected. And after solvent evaporation under reduced pressure, the crude product was purified by silica gel column chromatography using hexane as eluent to give the targeted product as colorless oil in 95% yield (2.02 g). ^{1}H-NMR (500 MHz, $CDCl_3$, ppm): 9.83 (s, 1H), 7.40 (d, $J = 8.2$ Hz, 2H), 6.90 (d, $J = 8.2$ Hz, 1H), 4.06 (m, 4H), 1.81 (m, 4H), 1.48 (s, 4H), 1.34 (s, 8H), 0.90 (s, 4H). MALDI-TOF (*m/z*): [M+] Calcd. $C_{19}H_{30}O_3$, 306.44; Found, 307.5.

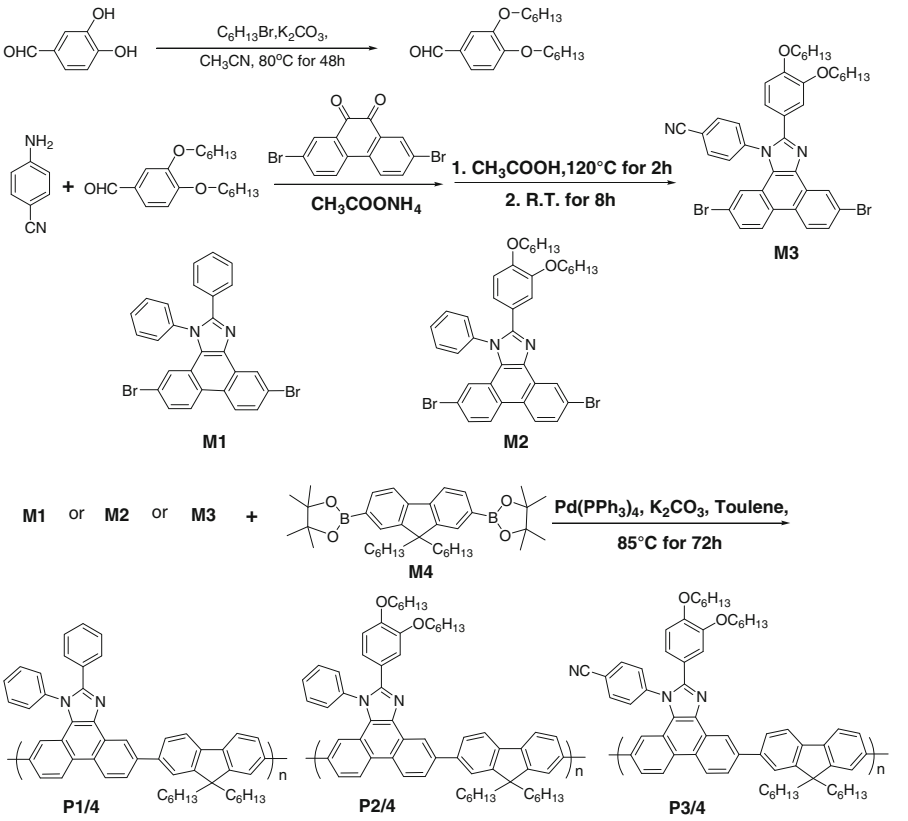

Scheme 1 Synthesis of **P1/4**, **P2/4**, and **P3/4** by palladium-catalyzed Suzuki coupling reaction of monomer **M4** with monomers **M1**, **M2**, and **M3**

*Preparation of 5,10-dibromo-1,2-diphenyl-1H-phenanthro[9,10-d]imidazole (**M1**)*

To a 250 mL round-bottom flask equipped with a stirrer were added 1.83 g (5.0 mmol) of 2,7-dibromophenanthrenequinone, 2.30 g (25.0 mmol) of aminobenzene, 0.53 g (5 mmol) of benzaldehyde, 1.54 g (20.0 mmol) of amino acetic acid and acetic acid (120 mL). After stirring for 2 h at 120 °C, the mixture was filtered and the precipitates were washed with dilute acetic acid. The filtrates were collected, and after solvent evaporation under reduced pressure, the crude product was purified by silica gel column chromatography using CH_2Cl_2 as eluent to give **M1** as white solid in 70% yield. ^{1}H NMR (500 MHz, $CDCl_3$, ppm): 9.02 (d, $J = 2.1$ Hz, 1H), 8.53 (d, $J = 8.8$ Hz, 1H), 8.47 (d, $J = 8.8$ Hz, 1H), 8.69 (dd, $J = 7.6$ Hz, 2.1 Hz, 1H), 7.70–7.62 (m, 3H), 7.61–7.55 (m, 3H), 7.50 (m, 2H), 7.37–7.28 (m, 3H), 7.20 (d, $J = 2.1$ Hz, 1H). MALDI-TOF (*m*/*z*): [M+] Calcd. $C_{27}H_{16}Br_2N_2$, 525.97; Found, 527.3. Anal Calc. for $C_{27}H_{16}Br_2N_2$: C, 61.39; H, 3.05; N, 5.30; Br, 30.25. Found: C, 61.20; H, 3.02; N, 5.31.

*Preparation of 2-(3,4-bis(hexyloxy)phenyl)-5,10-dibromo-1-phenyl-1H-phenanthro[9,10-d]imidazole (**M2**)*

To a 250 mL round-bottom flask equipped with a stirrer were added 1.83 g (5.0 mmol) of 2,7-dibromophenanthrenequinone [35], 2.30 g (25.0 mmol) of aminobenzene, 1.65 g (5 mmol) of **M1**, 1.54 g (20.0 mmol) of amino acetic acid, and acetic acid (80 mL). After stirring for 12 h at 120 °C, the mixture was added 2 mL of water. The mixture was then filtered and the precipitates were washed with dilute acetic acid. The crude product was purified by silica gel column chromatography using CH_2Cl_2 as eluent to give **M2** as white solid in 80% yield. ^{1}H NMR (500 MHz, $CDCl_3$, ppm): 8.98 (s, 1H), 8.45 (d, $J = 8.80$ Hz, 1H), 8.39 (d, $J = 8.80$ Hz, 1H), 7.65 (dd, $J = 8.8$ Hz, 2.10 Hz, 1H), 7.62–7.56 (m, 3H), 7.50 (dd, $J = 8.80$ Hz, 2.1 Hz, 1H), 7.48–7.42 (m, 2H), 7.14–7.09 (m, 2H), 7.03 (s, 1H), 6.72 (d, $J = 8.50$ Hz, 1H), 3.91 (t, $J = 6.7$ Hz, 7.00 Hz, 2H), 3.72 (t, $J = 6.70$ Hz, 7.0 Hz, 2H), 1.73–1.68 (m, 4H), 1.44–1.21 (m, 12H), 0.89–0.79 (m, 6H). MALDI-TOF (*m*/*z*): [M+] Calcd. $C_{39}H_{40}Br_2N_2O_2$, 726.15; Found, 727.3. Anal Calc. for $C_{39}H_{40}Br_2N_2O_2$: C, 64.29; H, 5.53; Br, 21.93; N, 3.85; O, 4.39. Found: C, 64.12; H, 5.39; N, 3.88, O, 4.36.

*Preparation of 4-(2-(3,4-bis(hexyloxy)phenyl)-5,10-dibromo-1H-phenanthro[9,10-d]imidazole-1-yl)benzonitrile (**M3**)*

To a 250 mL round-bottom flask equipped with a stirrer were added 1.83 g (5.0 mmol) of 2,7-dibromophenanthrenequinone, 3.00 g (25.0 mmol) of cyanoaminobenzene, 1.60 g (5 mmol) of 3,4-bis(hexyloxy)benzaldehyde, 1.54 g (20.0 mmol) of amino acetic acid and acetic acid (120 mL). After stirring for 12 h at 120 °C, the mixture was added 5 mL of water. The mixture was then filtered and the precipitates were washed with dilute acetic acid. The crude product was purified by silica gel column chromatography using CH_2Cl_2 as eluent to give **M3** as white solid in 70% yield. ^{1}H NMR (500 MHz, $CDCl_3$, ppm): 8.99 (d, $J = 2.10$ Hz, 1H), 8.53 (d, $J = 8.80$ Hz, 1H), 8.45 (d, $J = 8.80$ Hz, 1H), 7.94 (d, $J = 8.50$ Hz, 2H), 7.73 (dd, $J = 8.80$ Hz, 2.10 Hz, 1H), 7.64 (d, $J = 8.50$ Hz, 1H), 7.60 (dd, $J = 8.80$ Hz, 2.1 Hz, 1H), 7.15 (d, $J = 2.10$ Hz, 1H), 7.09 (d, $J = 2.10$ Hz, 1H), 6.87 (dd, $J = 8.20$ Hz, 2.1 Hz, 1H), 6.75 (d, $J = 8.20$ Hz, 1H), 4.00 (t, $J = 6.70$ Hz, 7.0 Hz, 2H), 3.88 (t, $J = 6.70$ Hz, 7.0 Hz, 2H), 1.86–1.74 (m, 4H), 1.51-1.41 (m, 4H), 1.40–1.29 (m, 8H), 0.96–0.86 (m, 6H). MALDI-TOF (*m*/*z*): [M+] Calcd. $C_{40}H_{39}Br_2N_3O_2$, 751.14; Found, 723.5. Anal Calc. for $C_{40}H_{39}Br_2N_3O_2$: C, 63.75; H, 5.22; Br, 21.21; N, 5.58; O, 4.25. Found: C, 63.52; H, 5.18; N, 5.77, O, 4.33.

Polymerization

All the polymerization reactions and manipulations were carried out under nitrogen, except for the purification of the polymers, which was done in open air. A typical experimental procedure for the polymerization of **M1** with **M4** is given below as an example. Into a baked 50 mL flask was added **M1** (180 mg, 0.34 mmol), **M4** (200 mg, 0.34 mmol), and $Pd(PPh_3)_4$ (9.30 mg, 0.008 mmol). The flask was

evacuated under vacuum for half an hour and then flushed with nitrogen. Freshly distilled toluene (1.2 mL) and 0.8 mL of 2 M K_2CO_3 aqueous solution were injected into the flask. After reflux under nitrogen for 72 h, the solution was cooled to room temperature, washed with 20 mL of water. The organic layer was extracted with chloroform and dried over $MgSO_4$. The mixture was then filtered and the filtrates were collected. After solvent evaporation under reduced pressure, it was precipitated in 150 mL methanol. After filtration, the polymer was dried in a vacuum oven at 40 °C to a constant weight. Yield: 72%. ^{1}H NMR (500 MHz, $CDCl_3$, ppm): 9.33–9.14 (br, m, PIM Ar–H, 1H), 8.94–8.55 (br, m, PIM Ar–H, 2H), 8.19–7.85 (br, m, PIM Ar–H, 3H and fluorene Ar–H, 2H), 7.53–7.28 (br, m, PIM Ar–H, 5H and fluorene Ar–H, 4H), 7.53–7.28 (br, m, PIM Ar–H, 5H), 2.27–1.92 (br, m, CH_2, 4H), 1.30–0.95 (br, m, CH_2, 12H), 0.95–0.55 (br, m, CH_2 and CH_3, 10 H). $M_n = 7.5 \times 10^3$, $M_w = 15.8 \times 10^3$, PD = 2.1. Anal. Calcd. for $(C_{52}H_{48}N_2)_n$: C, 89.10; H, 6.90; N, 4.00. Found: C, 85.24; H, 5.08; N, 3.86.

Other polymers are prepared by the similar procedure and their characterization data are given below. **PF** was synthesized to compare the properties with these PI-containing polymers.

P2/4

^{1}H NMR(500 MHz, $CDCl_3$, ppm): 9.34–9.16 (br, m, PIM Ar–H, 1H), 8.98–8.59 (br, m, PIM Ar–H, 2H), 8.13–7.83 (br, m, PIM Ar–H, 3H and fluorene Ar–H, 2H), 7.82–7.53 (br, m, PIM Ar–H, 4H and fluorene Ar–H, 4H), 7.53–7.29 (br, m, PIM Ar–H, 2H), 7.17–7.03 (br, m, PIM Ar–H, 1H), 6.90–6.73 (br, m, PIM Ar–H, 1H), 4.10–3.90 (br, m, PIM Ar–OCH_2, 2H), 3.90–3.63 (br, m, PIM Ar–OCH_2, 2H), 2.31–1.92 (br, m, CH_2, 4H), 1.89–1.68 (br, m, CH_2, 4H), 1.59–1.22 (br, m, CH_2, 12H),1.27–0.98 (br, m, CH_2, 12H), 0.98–0.49 (br, m, CH_2 and CH_3, 16H). $M_n = 21.0 \times 10^3$, $M_w = 58.8 \times 10^3$, PD = 2.7. Anal. Calcd. for $(C_{64}H_{72}N_2O_2)_n$: C, 85.29; H, 8.05; N, 3.11; O, 3.55. Found: C, 82.69; H, 6.98; N, 2.99; O, 3.35.

P3/4

^{1}H NMR(500 MHz, $CDCl_3$, ppm): 9.26–9.15 (br, m, PIM Ar–H, 1H), 8.97–8.62 (br, m, PIM Ar–H, 2H), 8.12–7.86 (br, m, PIM Ar–H, 4H and fluorene Ar–H, 2H), 7.86–7.57 (br, m, PIM Ar–H, 1H and fluorene Ar–H, 4H), 7.51–7.29 (br, m, PIM Ar–H, 2H), 7.17–7.07 (br, m, PIM Ar–H, 1H), 7.02–6.92 (br, m, PIM Ar–H, 1H), 6.85–6.72 (br, m, PIM Ar–H, 1H), 4.09–3.96 (br, m, PIM Ar–OCH_2, 2H), 3.94–3.81 (br, m, PIM Ar–OCH_2, 2H), 2.36–1.91 (br, m, CH_2, 4H), 1.90–1.65 (br, m, CH_2, 4H), 1.62–1.22 (br, m, CH_2, 12H), 1.21–0.97 (br, m, CH_2, 12H), 0.96–0.53 (br, m, CH_2 and CH_3, 16H). $M_n = 21.8 \times 10^3$, $M_w = 48.8 \times 10^3$, PD = 2.2. Anal. Calcd. for $(C_{65}H_{71}N_3O_2)_n$: C, 84.28; H, 7.73; N, 4.54; O, 3.45. Found: C, 82.09; H, 7.06; N, 4.32; O, 3.07.

PF

^{1}H NMR (500 MHz, $CDCl_3$, ppm): 7.91–7.75 (br, m, fluorene Ar–H, 2H), 7.76–7.50 (br, m, fluorene Ar–H, 4H), 2.27–1.92 (br, m, CH_2, 4H), 1.30–0.95 (br, m,

CH_2, 12H), 0.95–0.55 (br, m, CH_2 and CH_3, 10H). ^{13}C NMR (125 MHz, $CDCl_3$): 154.81, 151.82, 140.55, 140.04, 136.56, 133.47, 129.59, 126.16, 121.55, 120.62, 119.97, 69.87, 55.34, 40.37, 31.40, 31.47, 29.68, 29.49, 29.16, 25.73, 23.86, 22.63, 22.56, 14.09, 14.02. $M_n = 10.8 \times 10^3$, $M_w = 20.6 \times 10^3$, PD = 1.9. Anal. Calcd. for $(C_{25}H_{32})_n$: C, 89.76; H, 10.24. Found: C, 86.90; H, 10.81.

Results and discussion

Monomer synthesis

To explore the properties of PI-containing polymers, we design the molecular structures of a series of functional monomers (**M1**–**M3**) as shown in Scheme 1. All three new monomers (**M1**–**M3**) are synthesized in one-pot reaction [40–43]. The mixture of aniline, phenanthrenequinone, ammonium acetate, and corresponding aromatic aldehyde are refluxed for 2 h, then cooled to room temperature and filtered. The crude product of light yellow powder is purified by chromatography and the yields of all target products are above 75%. All the monomers are characterized by standard spectroscopic methods, from which satisfactory data corresponding to their molecular structures are obtained.

Polymerization

After obtaining the monomers, we then try to polymerize them by $Pd(PPh_3)_4$, a commonly used catalyst for Suzuki coupling reaction [44, 45]. Reaction of **M1** with **M4** in the presence of $Pd(PPh_3)_4$ in refluxed toluene gives a high-molecular weight polymer with a reasonably high yield (Table 1). Under the same conditions, **M4** reacted with **M2** and **M3**, respectively, producing **P2/4** and **P3/4** with M_w's from 58,800 to 48,800 in 60–72% yields. **P2/4** and **P3/4** show higher molecular weights than **P1/4** because the solubility of **M2** and **M3** are better than **M1** after being attached with the long alkoxyl side chain [46]. All these polymers were readily dissolved in common organic solvents, such as THF, $CHCl_3$, toluene, and DMF.

Structural characterization

The polymeric products were characterized spectroscopically. All the polymers give satisfactory analysis data corresponding to their expected molecular structures. An IR spectrum of **P3/4** is shown in Fig. 1 as an example. For comparison, the spectra of its monomers **M3** and **M4** are also provided in the same figure. The band at 2,200/cm associated with CN stretching is clearly seen in the spectrum of the monomer **M3**, which is also observed in the spectrum of **P3/4**, indicating that the CN group has been introduced into the new formed polymer. The boron ester stretching vibration at 1,350/cm of **M4** almost disappears after polymerization. Meanwhile, the absorption band of alkyl side chain and alkoxyl side chain at 3,100–2,800/cm are all observed in these three spectra. All these spectral data prove that monomers **M3** and **M4** have been successfully transformed to polymer **P3/4**.

Table 1 The molecular weight, thermal, absorption, and emission characteristics of **PF**, **P1/4**, **P2/4**, and **P3/4** in solution and film states

	M_n ($\times 10^3$)	M_w ($\times 10^3$)	PD	T_d[a] (°C)	T_g (°C)	In THF (nm)		Φ_{fl}[b] (%)	In solid (nm)	
						Abs	PL		Abs	PL
PF	10.8	20.6	1.9	331	96	375	418(440)	75	380	425(450)
P1/4	7.5	15.8	2.1	397	207	368(311)	440(418)	88	378(309)	450(425)
P2/4	21.0	58.8	2.7	415	189	378(315)	440(418)	90	385(310)	450(425)
P3/4	21.8	48.8	2.2	397	195	380(308)	418(440)	92	388(310)	425(451)

[a] The temperature for 5% weight loss of the polymers

[b] The fluorescence quantum yield in THF solution using 0.1 M H_2SO_4 solution of quinine as reference (0.54)

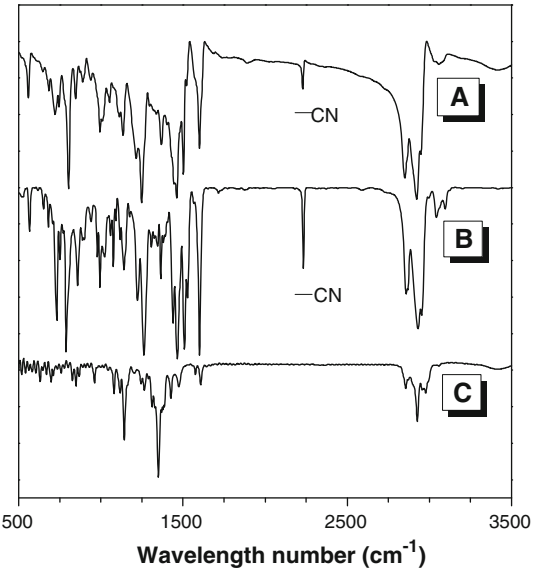

Fig. 1 IR spectra of (*A*) polymer **P3/4**, (*B*) monomer **M3**, and (*C*) monomer **M4**

Similar results were obtained from the NMR analyses. Figure 2 shows the ^{1}H NMR spectra of **P3/4** and its monomer **M3** and **M4**. In the spectrum of **M3**, the absorptions of the CH_2 protons linked with oxygen atom on the side chain are observed at 3.60 and 4.00 ppm, and **P3/4** shows the similar proton resonances in this area. Compared with our earlier study, these are assigned to the typical resonances of PI group, although they become weaker in **P3/4**. In the area of 6.50–7.26 ppm, four absorptions of protons are observed in **M3**, while in **P3/4** the number is decreased to three peaks because the other one moves to low field region. All this proved that the **M3** block is inserted to the **P3/4** polymer. The evidence of **M4** linked to the backbone in **P3/4** originates from the response around 2.00 ppm as observed in the other polyfluorenes derivatives [36, 37]. From 7.26 to 8.50 ppm, the absorptions of the aromatic fluorene hydrogen and aromatic phenanthrene hydrogen of **P3/4** are hard to distinguish, presumably due to their overlapping. In short, no unexpected peaks are found, and all the peaks can be readily assigned. Thus, the polymeric product is indeed **P3/4** with a

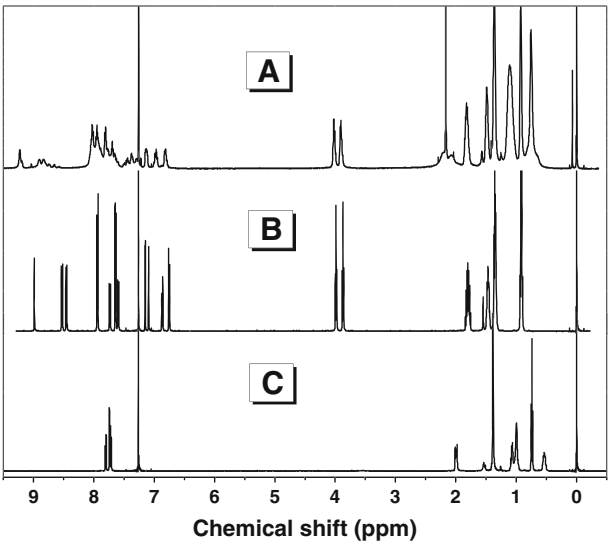

Fig. 2 ^{1}H NMR spectra of $CHCl_3$-*d* solutions of (*A*) polymer **P3/4**, (*B*) monomer **M3**, and (*C*) monomer **M4**

molecular structure as shown in Scheme 1. Similar observations are found in the spectra of **P1/4** and **P2/4**, respectively.

Thermal stability

The thermal stability of the polymers is evaluated by TGA analysis. As shown in Fig. 3, all the polymers are thermally stable, losing 5% of their weights (T_d) at 397–415 °C (Table 1), which are much higher than that of polyfluorene (331 °C). The high T_d values of the polymers are understandable because they are constructed from aromatic rings, which possess a high resistance to thermolysis. More importantly, these polymers could form amorphous films with high-glass transition temperature (T_g) of 207, 189, and 195 °C, respectively, which are distinctly higher than that of **PF** (96 °C) (Fig. 4). Such high-T_g values implicate that they could form morphologically stable amorphous films upon thermal evaporation, which is highly important for application in OLEDs. At the same, it is proved that the PI unit is a good block to increase the materials thermal stability from oligomer to polymer. **P1/4** shows the highest T_g due to its more rigid structure.

To investigate the fluorescence stability of the polymers in the solid state, we performed annealing experiments. The solid films of these polymers were first baked at 60 °C for 30 min in air, then at 180 °C for another 30 min, followed by 240 °C. **P3/4** shows very good spectra stability. Figure 5 showed the normalized PL emission spectra of the **P3/4** after annealing in air. It was reported that thermal treatment of the film of poly(dihexylfluorene) at 100 °C would lead to a significant increase in the shoulder peak centered at 460 nm because of the aggregation effect or keto formation in air [47]. However, **P3/4** was very stable even after baking at 180 °C for 0.5 h, and the PL spectra were almost the same as those tested before annealing. Accompanying

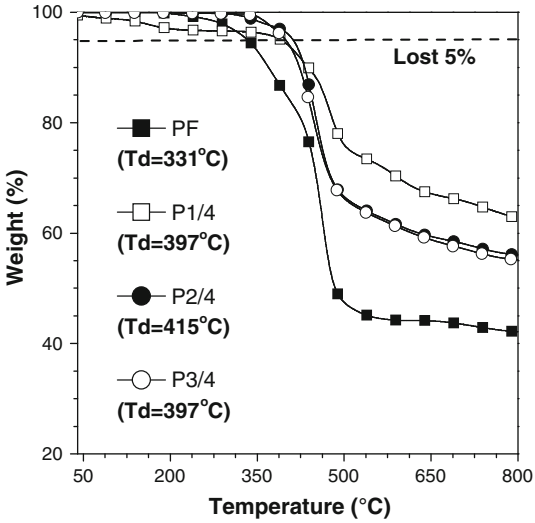

Fig. 3 TGA thermograms of **P1/4**, **P2/4**, **P3/4**, and **PF** recorded under nitrogen at a heating rate of 20 °C/min

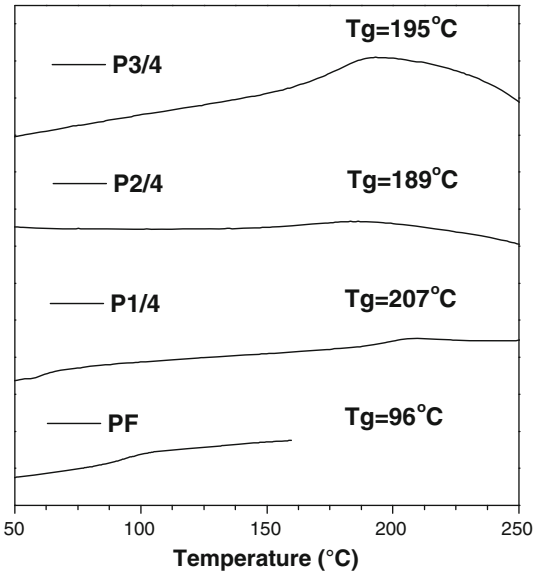

Fig. 4 DSC thermograms of **P1/4**, **P2/4**, **P3/4**, and **PF** measured at a scan rate 10 °C/min under nitrogen

the further increased temperature, there appeared a new shoulder peak at ~520 nm, which was not apparent after annealing at 180 °C for another 0.5 h, suggesting that bulky structure resulted in better spectra-thermal stability, and the formation of aggregation excimer and keto defects were effectively suppressed.

Absorption and emission

Figure 6 shows the UV spectra of the polymers in their dilute solutions in THF. All these polymers exhibit their maxima absorption peaks around 365–380 nm, which

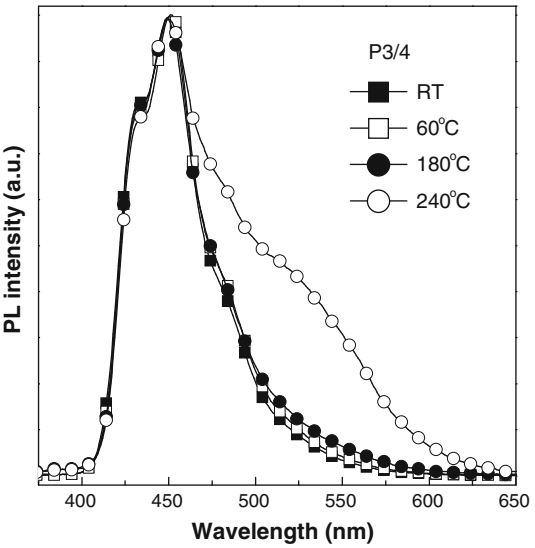

Fig. 5 PL spectra of the films of **P3/4** before and after annealing at different temperatures for 30 min in air

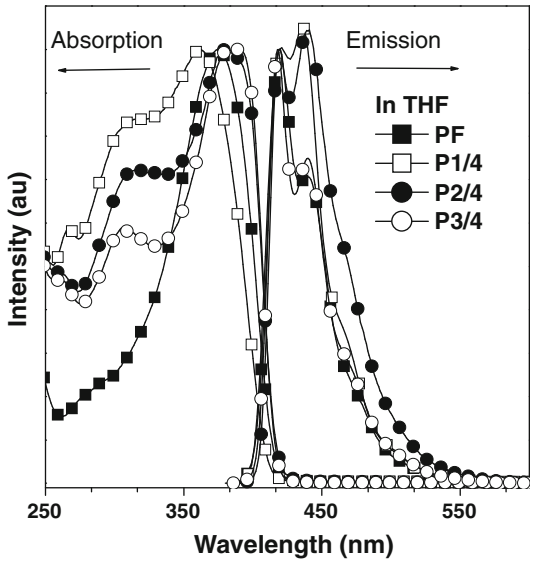

Fig. 6 Normalized UV and PL spectra of THF solutions of **P1/4**, **P2/4**, **P3/4**, and **PF**. Concentration: 10 μM. Excitation wavelength: 370 nm

are due to the π–π^* transitions of the polymer backbones. The new absorption peak at 310 nm, which is not observed in **PF** but in the three PI-containing polymers, is assigned to the new formed imidazole ring. Compared to their inherent monomers, their absorption peaks are all red-shifted to longer wavelengths. For example, **P3/4** absorbs at 310 nm and 385 nm, which are red-shifted from those of **M3** and **M4** by 37 and 22 nm, respectively. This indicates a more extended electronic conjugation in the polymer system because of the electronic communication between the aromatic chromophoric units. The emission of **PF** shows main peaks at 418 nm and a shoulder peak at 440 nm. When the PI group are introduced into the **PF** backbone,

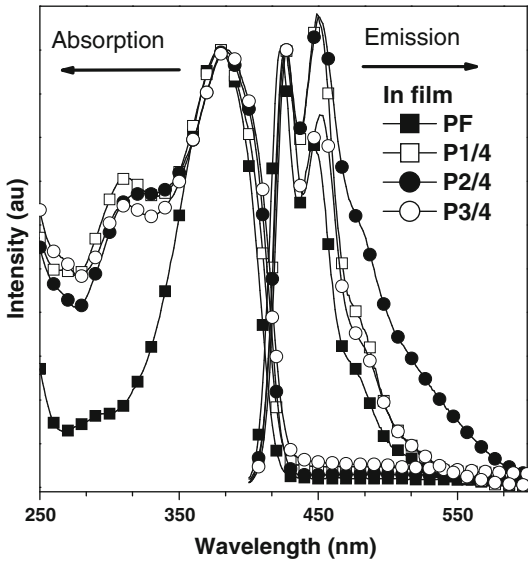

Fig. 7 Normalized UV and PL spectra of **P1/4**, **P2/4**, **P3/4**, and **PF** in film state. Concentration: 10 μM. Excitation wavelength: 370 nm

P1/4 and **P2/4** exhibit the same emission peaks which mean that there is no energy transfer between the fluorene and PI units and insures the high efficiencies of these polymers. While the intensity of emission peak at 440 nm is higher than the peak at 418 nm, which might be due to the change of the polymer configuration by the imidazole ring and the long alkoxyl side chains. **P3/4** shows the same emission as that of **PF** because the electron-withdrawing effect and steric hindrance of cyano group which stabilizes the phenyl ring at 1-N position and suppresses the interactions between the long alkoxyl side chains. **P1/4**, **P2/4**, and **P3/4** all show higher quantum efficiencies than **PF** in dilute solution as summarized in Table 1.

The absorption and emission spectra of the polymers as thin film in solid state are shown in Fig. 7. All the polymers show very similar absorption spectra with main peak at 380 nm, which are a little bit red-shifted compared with their solutions. The absorption peaks of imidazole ring at 310 nm for **P1/4**, **P2/4**, and **P3/4** are all observed. All their emission spectra in solid state peak at 425 and 450 nm, showing 10 nm red shift compared with their solutions, respectively. The emission spectra of **P2/4** are broader than the other two both in solution and in solid state due to interactions between the long alkoxyl side chains. Because of the electron-withdrawing effect and steric hindrance of cyano group as mentioned above, **P3/4** shows similar profiles as that of **P1/4** both in solution and in solid state.

Electrochemistry properties

Electronic structures (HOMO and LUMO) are characterized by CV using a glass carbon disk ($\Phi = 3$ mm) as working electrode, platinum wire as auxiliary electrode, and Ag/Ag^+ as reference electrode. As shown in Fig. 8, CV analysis for **P1/4** exhibits one quasi-reversible oxidation wave with an oxidative onset potential of 0.84 V, which gives a HOMO level of −5.55 eV by comparison to ferrocene ($E_{HOMO} = -(eE_{ox} + 4.71$ eV))

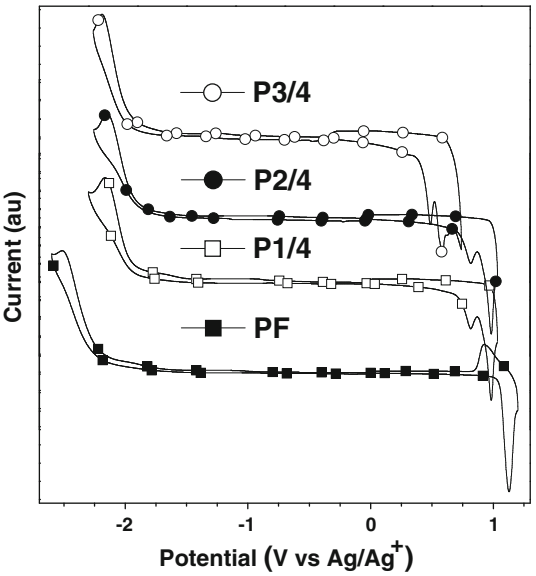

Fig. 8 Cyclic voltammogram of **PF**, **P1/4**, **P2/4**, and **P3/4**

Table 2 The electrochemistry and device data of **PF**, **P1/4**, **P2/4**, and **P3/4**

	HOMO[a] (eV)	LUMO (eV)	E_{gap}[b] (eV)	Voltage[c] (V)	L_{max} (cd/m^2)	LE_{max} (cd/A)	EQE_{max} (%)
PF	−5.75	−2.45	3.30	15.0	18	0.012	0.015
P1/4	−5.55	−2.55	3.00	12.7	420	0.077	0.096
P2/4	−5.56	−2.58	2.98	12.5	71	0.15	0.18
P3/4	−5.59	−2.63	2.96	7.2	1,200	0.13	0.20

[a] Calculated by comparing with ferrocene (Fc) (4.8 eV) and calibrated using $E_{1/2}$ (Fc/Fc^+) = 0.09 V

[b] Calculated from the electrochemistry data

[c] Device structure: ITO/PEDOT:PSS (40 nm)/PVK (≈40 nm)/polymer (≈50 nm)/LiF (0.5 nm)/Al (100 nm); the turn-on voltage ($L > 1$ cd/m^2)

[48, 49]. The HOMO levels of **P2/4** and **P3/4** are measured to be −5.56 and −5.59 eV, respectively (Table 2). The HOMO levels of these PI-based polymers are similar, which are elevated 0.16–0.20 eV compared to that of **PF** (HOMO level of −5.75 eV), indicating a decreased holes injection barrier. The CV analysis gives the LUMO levels of −2.55, −2.58, and −2.63 eV for **P1/4**, **P2/4**, and **P3/4**, respectively. **P3/4** shows the lowest LUMO level because of the electron-withdrawing cyano group, which are 0.18 eV lower than that of **PF** (LUMO level of −2.45 eV), revealing that the electrons injection barrier is also decreased. This reflects the more balanced carrier injection properties in these PI-based polymers, especially for **P3/4**.

Device performance

To evaluate the potential application of these compounds in blue PLEDs, we fabricate the device with a configuration of ITO/PEDOT:PSS (40 nm)/PVK

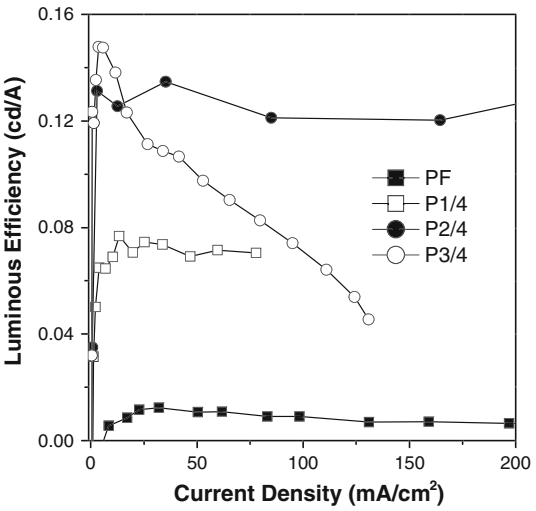

Fig. 9 The luminous efficiency of **P1/4**, **P2/4**, and **P3/4** compared with **PF**. Device structure: ITO/PEDOT:PSS (40 nm)/PVK (40 nm)/polymer (50 nm)/LiF (0.5 nm)/Al (100 nm)

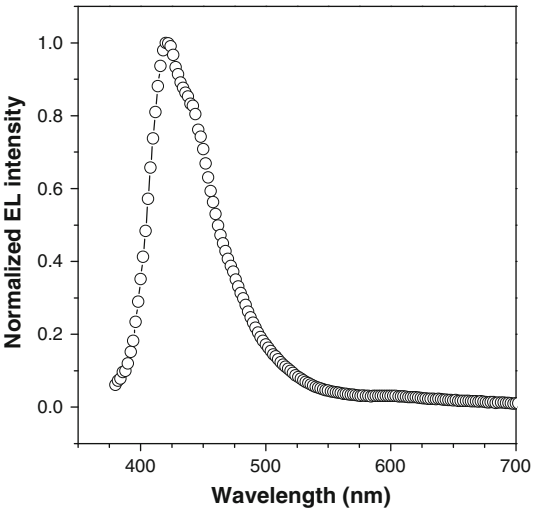

Fig. 10 Electroluminescent spectrum of **P3/4**. Device structure: ITO/PEDOT:PSS (40 nm)/PVK (40 nm)/polymer (50 nm)/LiF (0.5 nm)/Al (100 nm)

(40 nm)/polymer (50 nm)/LiF (0.5 nm)/Al (100 nm). **P1/4**, **P2/4**, and **P3/4** all show higher maximum luminous efficiencies than **PF**, and the turn-on voltages ($L > 1$ cd m^{-2}) all become lower than **PF** (Fig. 9). This is because the carriers injection barriers are decreased, which is consistent with the results revealed by CV. The device based on **P3/4** exhibits better performance with a lower turn-on voltage of 7.2 V, a maximum luminance of 1,200 cd/m^2, a maximum luminous efficiency of 0.13 cd/A and an external quantum efficiency of 0.2%. As can be seen in Fig. 10, the electroluminescence locates in the deep blue region with main peak at 425 nm with a CIE coordinate of (0.17, 0.08), which is corresponded to its emission in solid state without red shift, indicating a good deep blue emission material. It also can be applied as host material for phosphorescence device. Better device performance

could be expected provided that they can be measured under a more advanced condition.

Conclusion

In summary, we have developed the PI building block for efficient blue light emitting materials. By inserting the alkoxyl side chain in PI unit, the molecular weight was improved. Comparing with a model polymer **PF**, the new-generated three blue polymers show comprehensive enhancement in the basic characteristics involving thermal stability, fluorescent efficiency, charge injection property and the performance in device. When the electron-withdrawing cyano group is introduced, the energy level of **P3/4** has been tuned to be easier for the carrier's injection. The device based on **P3/4** shows better performance than **PF**, **P1/4**, and **P2/4**. The electroluminescence locates in the deep blue region with a CIE coordinate of (0.17, 0.08) and the external efficiency of the device could reach to 0.2%. The work demonstrates that PI unit is a good block to construct deep blue emission materials, and it indicates the chemical structure modification could improve material's properties.

Acknowledgments We are grateful for support from the National Science Foundation of China (Grant Nos. 20704016, 21174050), the Ministry of Education of China (Grant No. 20070183202).

References

1. Burroughes JH, Bradley DDC, Brown AR (1990) Light-emitting diodes based on conjugated polymers. Nature 347:539
2. Braun D, Heeger AJ (1991) Visible light emission from semiconducting polymer diodes. Appl Phys Lett 58:1982
3. Hebner TR, Wu CC, Marcy D, Lu MH, Sturm JC (1998) Ink-jet printing of doped polymers for organic light emitting devices. Appl Phys Lett 72:519
4. Chang SC, Liu J, Bharathan J, Yang Y, Onohara J, Kido J (1999) Multicolour organic light-emitting diodes processed by hybrid inkjet printing. Adv Mater 11:734
5. Fu YQ, Li Y, Li J, Yan SK, Bo ZS (2004) High molecular weight dendronized poly(fluorene)s with peripheral carbazole groups: synthesis, characterization, and properties. Macromolecules 37:6395
6. Luo J, Peng J, Cao Y, Hou Q (2005) High-efficiency red light-emitting diodes based on polyfluorene copolymers with extremely low content of 4,7-di-2-thienyl-2,1,3-benzothiadiazole-comparative studies of intrachain and interchain interaction. Appl Phys Lett 87:261103
7. Pu YJ, Higashidate M, Nakayama KI, Kido J (2008) Solution-processable organic fluorescent dyes for multicolor emission in organic light emitting diodes. J Mater Chem 18:4183
8. Zhang Y, Boer BD, Blom PWM (2009) Controllable molecular doping and charge transport in solution-processed polymer semiconducting layers. Adv Funct Mater 19:1901
9. Lu P, Zhang HQ, Shen FZ, Yang B, Li D, Ma YG (2003) A wide-bandgap semiconducting polymer for ultraviolet and blue light emitting diodes. Macromol Chem Phys 204:2274
10. Levermore PA, Jin R, Wang XH, Mello JC, Bradley DDC (2009) Organic light-emitting diodes based on poly(9,9-dioctylfluorene-co-bithiophene) (F8T2). Adv Funct Mater 19:950
11. Yang RQ, Tian RY, Yan JG, Zhang Y, Yang J, Hou Q (2005) Deep-red electroluminescent polymers: synthesis and characterization of new low-band-gap conjugated copolymers for light-emitting diodes and photovoltaic devices. Macromolecules 38:244
12. Yu CY, Chen CP, Chan SH, Hwang GW, Ting C (2009) Thiophene/phenylene/thiophene-based low-bandgap conjugated polymers for efficient near-infrared photovoltaic applications. Chem Mater 21:3262

13. Jin Y, Kim Y, Kim SH, Song S, Woo HY, Lee K, Suh H (2008) Novel green-light-emitting polymers based on cyclopenta[def]phenanthrene. Macromolecules 41:5548
14. Zhen CG, Chen ZK, Liu QD, Dai YF, Shin RYC, Chang SY, Kieffer J (2009) Fluorene-based oligomers for highly efficient and stable organic blue-light-emitting diodes. Adv Mater 21:2425
15. Jeon SO, Jang SE, Son HS, Lee JY (2011) External quantum efficiency above 20% in deep blue phosphorescent organic light-emitting diodes. Adv Mater 23:1436
16. Huang CW, Peng KY, Liu CY, Jen TH, Yang NJ, Chen SA (2008) Creating a molecular-scale graded electronic profile in a single polymer to facilitate hole injection for efficient blue electroluminescence. Adv Mater 20:3709
17. Tseng SR, Li SY, Meng HF (2007) High-efficiency blue multilayer polymer light-emitting diode based on poly9,9-dioctylfluorene. J Appl Phys 101:084510
18. Lee TW, Kim MG, Kim SY, Park SH, Kwon O, Noh T, Oh TS (2006) Hole-transporting interlayers for improving the device lifetime in the polymer light-emitting diodes. Appl Phys Lett 89:123505
19. Kulkarni AP, Tonzola CJ, Babel A, Jenekhe SA (2004) Electron transport materials for organic light-emitting diodes. Chem Mater 16:4556
20. Strohriegl P, Grazulevicius JV (2002) Charge-transporting molecular glasses. Adv Mater 14:1439
21. Shirota Y, Kageyama H (2007) Charge carrier transporting molecular materials and their applications in devices. Chem Rev 107:953
22. Miteva T, Meisel A, Knoll W, Nothofer HG, Scherf U, Muller DC, Meerholz K, Yasuda A, Neher D (2001) Improving the performance of polyfluorene-based organic light-emitting diodes via end-capping. Adv Mater 13:565
23. Hung MC, Chen SA, Chen SH, Su AC (2005) Blue-emitting poly(2,7-pyrenylene)s: synthesis and optical properties. J Am Chem Soc 127:14576
24. Kawano S, Yang C, Ribas M, Baluschev S, Baumgarten M, Mullen K (2008) Blue-emitting poly(2,7-pyrenylene)s: synthesis and optical properties. Macromolecules 41:7933
25. Saleh M, Park Y, Baumgarten M, Kim J, Mullen K (2009) Conjugated triphenylene polymers for blue OLED devices. Macromol Rapid Commun 30:1279
26. Morin JF, Leclerc M, Ades D, Siove A (2005) Polycarbazoles: 25 years of progress. Macromol Rapid Commun 26:761
27. Lu JP, Tao Y, Diorio M, Li YN, Ding JF, Day M (2004) Pure deep blue light-emitting diodes from alternating fluorene/carbazole copolymers by using suitable hole-blocking materials. Macromolecules 37:2442
28. Wu FI, Shih PI, Shu CF, Tung YL, Chi Y (2005) Highly efficient light-emitting diodes based on fluorene copolymer consisting of triarylamine units in the main chain and oxadiazole pendent groups. Macromolecules 38:9028
29. Chien CH, Shih P, Wu FI, Shu CF, Yun C (2007) Polyfluorene presenting dipolar pendent groups and its application to electroluminescent devices. J Polym Sci A 45:2073
30. Zhu Y, Gibbons KM, Kulkarni AP, Jenekhe SA (2007) Polyfluorenes containing dibenzo[a,c]phenazine segments: synthesis and efficient blue electroluminescence from intramolecular charge transfer states. Macromolecules 40:804
31. Jenekhe SA, Lu L, Alam MM (2001) New conjugated polymers with donor-acceptor architectures: synthesis and photophysics of carbazole–quinoline and phenothiazine–quinoline copolymers and oligomers exhibiting large intramolecular charge transfer. Macromolecules 34:7315
32. Chen CH, Huang WS, Lai MY, Tsao WC, Lin JT, Wu YH, Ke TH, Chen LY, Wu CC (2009) Versatile, benzimidazole/amine-based ambipolar compounds for electroluminescent applications: single-layer, blue, fluorescent OLEDs, hosts for single-layer. Phosphorescent OLEDs. Adv Funct Mater 19:2661
33. Shi J, Tang CW, Chen CH (1997) US Patent No. 5,646,948
34. Lo SC, Male NAH, Markham JPJ, Magennis SW, Burn PL, Salata OV, Samuel IDW (2002) Green phosphorescent dendrimer for light-emitting diodes. Adv Mater 14:975
35. Wang ZM, Lu P, Chen SM, Gao Z, Shen FZ, Zhang WS, Xu YX, Kwok HS, Ma YG (2011) Phenanthro[9,10-*d*]imidazole as a new building block for blue light emitting materials. J Mater Chem 21:5415
36. Lu P, Zhang HQ, Shen FZ, Yang B, Li D, Ma YG, Chen XF, Li JH, Tamai N (2003) A wide-bandgap semiconducting polymer for ultraviolet and blue light emitting diodes. Macromol Chem Phys 204:2274
37. Wang HP, Lu P, Wang BL, Qiu S, Liu MR, Hanif M, Cheng G, Liu SY, Ma YG (2007) A water-soluble π-conjugated polymer with up to 100 mg/mL solubility. Macromol Rapid Commun 28:1645

38. Muddasir H, Lu P, Li M, Zheng Y, Xie ZQ, Ma YG, Li D, Li JH (2007) Synthesis, characterization, electrochemistry and optical properties of a novel phenanthrenequinone-alt-dialkylfluorene conjugated copolymer. Polym Int 56:1507
39. Wang ZM, Lu P, Zhang WS, Shen FZ, Hanif M, Ma YG (2009) Dual tuning of emission color and electron injection properties through in situ chemical reaction in a conjugated polymer containing 9,10-phenanthrenequinone. Macromol Chem Phys 23:2029
40. Grisorio R, Suranna GP, Mastrorilli P, Nobile CF (2007) A versatile synthesis for new 9,10-bis(4-alkoxyphenyl)-2,7-diiodophenanthrenes: useful precursors for conjugated polymers. Org Lett 9:3149
41. Chang YT, Hsu SL, Su MH, Wei KH (2007) Soluble phenanthrenyl-imidazole-presenting regioregular poly(3-octylthiophene) copolymers having tunable bandgaps for solar cell applications. Adv Funct Mater 17:3326
42. Chang YT, Hsu SL, Chen GY (2008) Intramolecular donor–acceptor regioregular poly(3-hexylthiophene)s presenting octylphenanthrenyl-imidazole moieties exhibit enhanced charge transfer for heterojunction solar cell applications. Adv Funct Mater 18:1
43. Chang YT, Hsu SL, Su MH, Wei KH (2009) Intramolecular donor–acceptor regioregular poly(-hexylphenanthrenyl-imidazole thiophene) exhibits enhanced hole mobility for heterojunction solar cell applications. Adv Mater 21:2093
44. Miyaura M, Suzuki A (1995) Palladium-catalyzed cross-coupling reactions of organoboron compounds. Chem Rev 95:2457
45. Remmers M, Schulze M, Wegner G (1996) Characterisation and properties of poly(2,5-dialkoxy-oligophenylen-vinylene)s, poly(2,5-dialkoxy-oligophenylen-acetylene)s and related light-emitting polymers. Macromol Rapid Commun 17:239
46. Wu YG, Li J, Fu YQ, Bo ZS (2004) Synthesis of extremely stable blue light emitting poly(spirobifluorene)s with Suzuki polycondensation. Org Lett 6:3485
47. Li ZA, Ye SH, Liu YQ, Yu G, Wu WB, Qin JG, Li Z (2010) New hyperbranched conjugated polymers containing hexaphenylbenzene and oxadiazole units: convenient synthesis and efficient deep blue emitters for PLEDs application. J Phys Chem B 114:9101
48. Tang S, Liu MR, Lu P, Xia H, Li M, Xie ZQ, Shen FZ, Gu C, Wang H, Yang B, Ma YG (2007) A molecular glass for deep-blue organic light-emitting diodes comprising a 9,9′-spirobifluorene core and peripheral carbazole groups. Adv Funct Mater 17:2869
49. Wang ZM, Lu P, Xue SF, Gu C, Lv Y, Zhu Q, Wang H, Ma YG (2011) A solution-processable deep red molecular emitter for non-doped organic red-light-emitting diodes. Dyes Pigments 91:356